

9th International Conference on Applied Energy, ICAE2017, 21-24 August 2017, Cardiff, UK

## Model-based optimal load control of inverter-driven air conditioners responding to dynamic electricity pricing

Maomao Hu, Fu Xiao\*

*Department of Building Services Engineering, The Hong Kong Polytechnic University, Kowloon, Hong Kong*

### Abstract

Dynamic electricity pricing provides a great opportunity for residential consumers to participate into demand response (DR) programs to reduce the electricity bills. The lack of automatic response to time-varying electricity prices is one of the challenges faced by the residential electric appliances. Most of the existing studies on DR of residential air conditioner (ACs) focus on the single-speed ACs, rather than the inverter-driven ACs which are more energy efficient and extensively installed in today's residential buildings. This paper presents a novel model-based optimal load scheduling method for residential inverter-driven ACs to realize automatic DR to the day-ahead dynamic electricity prices. The models of the inverter-driven ACs and room thermal dynamics are firstly developed, identified and integrated for the development of the model-based scheduling. The tradeoff problem between the electricity costs, resident's comfort and peak power reductions is formulated as a mixed-integer nonlinear programming problem with adjustable weightings. The optimal solution of the nonlinear programming problem is searched by the genetic algorithm (GA). Simulation results show that multiple goals can be achieved via GA optimization and the regulations of the weights in the objective function. The developed framework can be implemented in the programmable communicating thermostats (PCTs) or the smart home energy manage systems (HEMSs) to enable residential inverter-driven ACs automatically respond to day-ahead dynamic electricity pricing.

© 2017 The Authors. Published by Elsevier Ltd.

Peer-review under responsibility of the scientific committee of the 9th International Conference on Applied Energy.

**Keywords:** Inverter-driven air conditioners; Demand response; Dynamic electricity pricing; Genetic algorithm; Mixed integer nonlinear programming

### 1. Introduction

In recent years, there has been a growing interest in demand response (DR) techniques due to its abilities to shift peak power demands, save the electricity costs and reduce the carbon emissions [1-4]. As indicated by Federal Energy Regulation Committee (FERC), the residential class will provide the largest DR resources, and the residential customers are able to provide over 45 percent of the total potential DR resources in 2019 [5]. Dynamic electricity pricing provides great opportunities for the residential consumers to participate into the DR programs for minimizing the electricity bills. Various time-varying electricity pricing schemes have been developed and implemented, such as time-of-use pricing (TOU), critical-peak pricing (CPP), real-time pricing (RTP), day-ahead pricing (DAP). Since residential air conditioners (ACs) are the major contributors to the home electricity bills, optimal load control for them can provide substantial economic benefits for return.

Recent studies have shown that one of the challenges faced by the residential electric appliances is the lack of the function of automatic response to the time-varying electricity prices. It is impractical for the common residents to manually and optimally manage the operations of residential ACs in response to the dynamic electricity prices. Thus, scheduling techniques should be developed to optimally and automatically respond to the dynamic electricity prices received from the electric utilities. The optimal scheduling algorithms for the residential ACs can be embedded in the programmable communicating thermostats (PCTs) or the smart home energy manage systems (HEMSs) to reduce the electricity bills while maintaining the comfort level. Thomas et al. [6] developed an intelligent AC controller which can provide optimal comfort and cost trade-offs for the residents during DR events. Chen et al. [7] evaluated the real-time price-based DR management for residential appliances via stochastic optimization and robust optimization. Li et al. [8] investigated and compared different DR strategies under the disturbances of dynamic pricing tariffs, seasons and weather based on eQUEST simulation. Molina et al. [9] combined model-predictive control and genetic algorithm to

\* Corresponding author. Tel.: +852 2766 4194; Fax: +852 2765 7198

E-mail address: [linda.xiao@polyu.edu.hk](mailto:linda.xiao@polyu.edu.hk)

regulate the residential temperature in the presence of dynamic electricity prices. However, the ACs used for optimal load scheduling in [6-9] are all single-speed ACs with on-off control algorithm. The present paper aims to optimally manage the loads of residential inverter-driven ACs based on the dynamic electricity prices using the evolutionary optimization technique of GA.

## 2. Model development

### 2.1. Inverter-driven AC model

Many studies have been devoted to the DR strategies of the single-speed ACs with the on-off control method. The single-speed ACs, however, are gradually replaced by the inverter-driven ACs which have gained an increasing market share in recent years due to its improved efficiency under part-load operating conditions. The residential ductless split-type inverter-driven ACs are studied in this paper to provide the DR resources during the DR events. In this paper, the physics-based modeling technique is used to obtain the typical performance data of inverter-driven ACs under typical environmental conditions and operating frequencies. For the purpose of simplification, only the four major components, i.e. condenser, evaporator, variable speed compressor, and electronic expansion valve (EEV), are modeled in this paper.

#### 2.1.1. Variable-speed compressor

Refrigerant mass flow rate and enthalpy at the compressor outlet are the key outputs of the compressor component. The refrigerant dynamics in the compressor can be represented by Eqs. (1) and (2).

$$\dot{m}_{comp} = N_{comp} V_{comp} \rho_{comp} \eta_v \quad (1)$$

$$h_{comp,o} = h_{comp,i} + (h_{comp,o,is} - h_{comp,i})/\eta_{is} \quad (2)$$

where  $N_{comp}$ ,  $V_{comp}$ ,  $\rho_{comp}$  are the rotational speed of compressor motor, effective displacement volume, refrigerant density at the inlet, respectively.  $h_{comp,i}$ ,  $h_{comp,o}$  are the enthalpies at the compressor inlet and outlet;  $h_{comp,o,is}$  is the enthalpy at the compressor outlet under an isentropic compression;  $\eta_v$  and  $\eta_{is}$  are the compressor volumetric efficiency and isentropic efficiency, respectively.

#### 2.1.2. Electronic expansion valve

The performance of expansion devices plays a critical role on the performances of inverter-driven ACs. They have been used in the refrigeration systems to regulate the refrigerant mass flow rate into the evaporator and maintain the refrigerant superheat at the evaporator outlet. In recent years, due to its superior performance in control, electronic expansion valves (EEV) have been implemented in the inverter air conditioners or heat pumps to control the cooling capacity and superheat instead of the conventional expansion devices such as capillary tubes and thermostatic expansion valves. The refrigerant dynamics in the EEV are shown in Eqs. (3) and (4).

$$\dot{m}_v = C_v A_v \sqrt{\rho_v (P_c - P_e)} \quad (3)$$

$$h_{v,o} = h_{v,i} \quad (4)$$

where  $C_v$ ,  $A_v$ ,  $\rho_v$  are the orifice coefficient, valve opening area, refrigerant density, respectively; and  $P_c$  and  $P_e$  are refrigerant pressures at the condenser and evaporator;  $h_{v,i}$  and  $h_{v,o}$  are the refrigerant enthalpies at the EEV inlet and outlet, respectively.

#### 2.1.3. Heat exchangers

Moving boundary approach has been widely adopted for both transient modeling [10, 11] and steady-state modeling [12, 13] of heat exchangers. The method is able to capture the characteristics of multiple fluid phase heat exchangers while preserving the simplicity of lumped parameter models. The condenser is normally divided into three zones based on the refrigerant state, i.e. de-superheated, two-phase, and subcooled zones, and the evaporator is divided into two zones, i.e. two-phase and superheated zones. With these assumptions, the one-dimensional steady state model of each zone can be represented by the conservation equations of mass and energy, which only contain the derivatives to the length of the zones. After integration along the length, the steady state model of a heat exchanger zone can then be transformed into the two algebraic equations as follows:

$$\dot{m}_{ex,o} = \dot{m}_{ex,i} \quad (5)$$

$$h_{ex,o} = h_{ex,i} + Q_{ref,air}/\dot{m}_{ex,i} \quad (6)$$

where  $\dot{m}_{ex,i}$  and  $\dot{m}_{ex,o}$  are the mass flow rates at the inlet and outlet of the zone, respectively;  $h_{ex,i}$  and  $h_{ex,o}$  are the enthalpy at the inlet and outlet of the zone, respectively;  $Q_{ref,air}$  is the heat exchanged between the refrigerant and the air in that zone (negative value for the condenser). The heat transfer rates,  $Q_{ref,air}$ , in heat exchangers are calculated by effectiveness-number of transfer units ( $\varepsilon$ -NTU).

### 2.2. Dynamic room thermal model

A room thermal model is required to characterize the room thermal dynamics and be integrated with the inverter-driven AC performance model for energy analysis. In our previous work [14, 15], an accurate resistance-capacitance (RC) room thermal model has been developed, identified, and validated. As shown in Fig. 1, the RC model mainly contains four parts, i.e. outdoor environment, building envelope, indoor air, and internal thermal mass. The energy balances for the external/internal wall surfaces, the indoor air and the internal thermal mass are given by Eqs. (7) - (10).

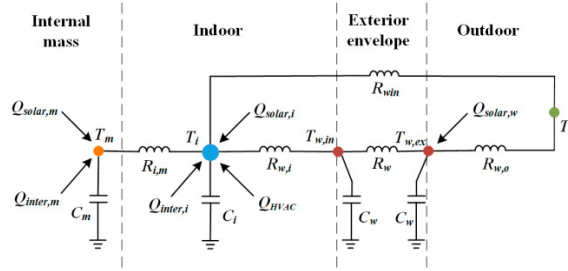


Fig. 1. Schematic of the grey-box thermal model of residential buildings.

$$C_w \frac{dT_{w,ex}}{dt} = \frac{T_o - T_{w,ex}}{R_{w,o}} + \frac{T_{w,in} - T_{w,ex}}{R_w} + Q_{solar,w} \quad (7)$$

$$C_w \frac{dT_{w,in}}{dt} = \frac{T_{w,ex} - T_{w,in}}{R_w} + \frac{T_i - T_{w,in}}{R_{w,i}} \quad (8)$$

$$C_i \frac{dT_i}{dt} = \frac{T_m - T_i}{R_{i,m}} + \frac{T_{w,in} - T_i}{R_{w,i}} + \frac{T_o - T_i}{R_{win}} + Q_{solar,i} + Q_{inter,i} + Q_{HVAC} \quad (9)$$

$$C_m \frac{dT_m}{dt} = \frac{T_i - T_m}{R_{i,m}} + Q_{solar,m} + Q_{inter,m} \quad (10)$$

where  $R$  and  $C$  represent the overall heat resistance and capacitance, respectively;  $T$  denotes temperature; subscripts  $i$ ,  $o$ ,  $w$ ,  $in$ ,  $ex$ ,  $win$  and  $m$  indicate indoor air, outdoor air, exterior wall, internal wall surface, external wall surface, window and internal mass, respectively;  $Q_{solar,w}$ ,  $Q_{solar,i}$  and  $Q_{solar,m}$  are solar heat gains absorbed by external wall surface, indoor air and internal mass, respectively;  $Q_{inter,i}$  and  $Q_{inter,m}$  are internal heat gains absorbed by indoor air and internal mass. Detail methods to calculate the  $Q_{solar}$  and  $Q_{inter}$  and the model identification algorithm can be found in our previous work [15].

### 2.3. Model integration

A room temperature controller plays the function of connecting the room thermal dynamics with the inverter-driven ACs. The inverter-driven AC controller in the present study is designed using a PID control structure. Fig. 2 depicts the block diagram for the frequency-based control of the inverter-driven AC system. After detecting the temperature difference from the set-point, the PID controller computes and outputs the actuating signal of rotational speed to the inverter-driven compressor. Under the specific compressor rotational speed and weather disturbances, the cooling capacity and COP of the inverter-driven AC can be determined using the developed AC model. The inverter-driven AC then delivers the cooling capacity into the air-conditioned room, removing the heat gains caused by the disturbances such as outdoor air temperature, solar radiation, and internal heat gains.

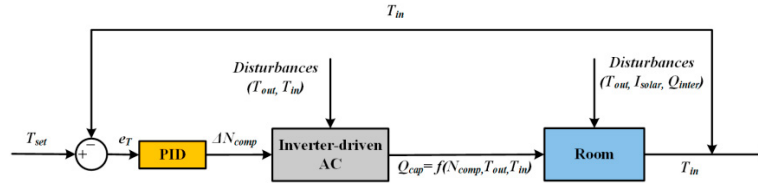


Fig. 2. Block diagram for the frequency control of the inverter-driven AC system.

### 2.4. Dynamic electricity pricing

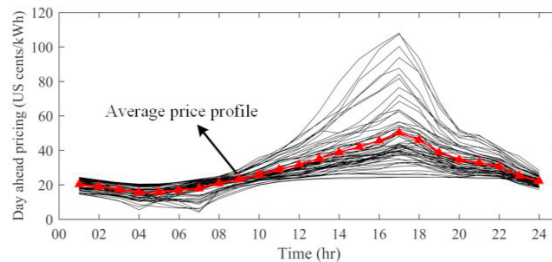


Fig. 3. Day ahead pricing data of the PJM energy market from June to July 2016.

Many electric utilities in the United States have implemented the DR programs via dynamic retail electricity prices. The real time pricing (RTP) and day ahead pricing (DAP) are the widely-used two types of dynamic electricity pricings by Independent System Operators (ISO) or Regional Transmission Operators (RTO) such as Electricity Reliability Council of Texas (ERCOT), PJM or New York ISO. Fig. 3 shows the historical DAP data of the PJM energy market from June to July 2016. The average DAP is used for the case study in this study.

### 3. Optimization problem formulation and solution

Given a set of temperature set-points, the daily profiles of indoor air temperature and power consumption can be obtained based on the developed integrated system. Both the dynamic room thermal model and the power consumption model of inverter-driven ACs are nonlinear models. Thus, the whole process of searching the optimal schedule of temperature set-points of the inverter-driven AC is formed as a mixed integer nonlinear programming problem. The objective of the optimization is to find the optimal schedule of temperature set-points, which make the objective function reach the minimal value.

#### 3.1. Problem formulation

The optimization performance is measured by the objective function as shown in Eq. (11), and the optimization aims to search the optimal set-point schedule ( $T_{set,1}, T_{set,2}, \dots, T_{set,k}$ ) to make the objective function reach the minimal value. The comprehensive objective ( $J^*$ ) consists three sub-objectives: the total energy cost ( $J_{cost}$  in Eq. (12)), the total comfort deviation ( $J_{comfort}$  in Eq. (13)), and the peak power consumption during the DR hours ( $J_{peak,DR}$  in Eq. (14)). The total energy consumption is the sum of the products of the hourly energy consumption of the inverter-driven AC ( $E_i$ ) and the hourly electricity price ( $C_i$ ). The total comfort deviation ( $J_{comfort}$ ) is the root mean square error (RMSE) of the indoor air temperatures to the expected temperature set-point. The peak power consumption is the maximal power consumption of the inverter-driven AC.  $\alpha$  and  $\beta$  represent the weights of thermal comfort and peak power, respectively. The time steps of the energy consumption ( $E_i$ ) and the electricity price ( $C_i$ ) are 1 hour and the time intervals of the indoor air temperature ( $T_{in,j}$ ) and the power consumption ( $P_i$ ) are both 1 minute. Besides, the optimization process should be subject to the model dynamics (Eq. (15) – (17)) and the comfort constraints (Eq. (18)) while searching the optimal solution.

$$\text{Minimize} \quad J^*(T_{set,1}, T_{set,2}, \dots, T_{set,k}) = J_{cost} + \alpha J_{comfort} + \beta J_{peak,DR} \quad (11)$$

$$J_{cost} = \sum_{i=1}^m E_i C_i; \quad (12)$$

$$J_{comfort} = \sqrt{\frac{1}{n} \sum_{j=1}^n (T_{in,j} - T_{in,exp,j})^2}; \quad (13)$$

$$J_{peak,DR} = \max\{P_1, P_2, \dots, P_l\}; \quad (14)$$

$$\text{Subject to} \quad J_{cost} = f(T_{set,1}, T_{set,2}, \dots, T_{set,k}, k) \quad (15)$$

$$J_{comfort} = g(T_{set,1}, T_{set,2}, \dots, T_{set,k}, k) \quad (16)$$

$$J_{peak,DR} = h(T_{set,1}, T_{set,2}, \dots, T_{set,k}, k) \quad (17)$$

$$T_{set,lb} \leq T_{set,k} \leq T_{set,ub} \quad (18)$$

#### 3.2. GA-based optimization

Conventional optimization technique depends strongly on the initial estimated values of the optimization problem and is usually possible to get a local optimal solution. The genetic algorithm (GA) is an evolutionary search algorithm inspired by the process of natural selection. It makes a population of individual solutions “evolve” toward an optimal solution by successive modifications. During each modification, three main types of rules, i.e. selection, crossover and mutation, are used to create the next generation from the current generation. The GA can address a variety of optimization problems that are not suitable for standard gradient descent methods, such as the problems in which the objective function is discontinuous, stochastic, or highly nonlinear. Some advantages of applying GA for this study are that the algorithm is gradient free and that the target problem is a mixed integer nonlinear programming problem. The GA is carried out in MATLAB, and performed on a desktop computer with Intel Core i7-4790 (3.60 GHz), 16 GB of memory, under Windows 10 64-bit operating system.

## 4. Results and discussions

### 4.1. Model parameter identification and validation

#### 4.1.1. Identification of the room thermal model

A residential room ( $L \times W \times H$ : 4.8m $\times$ 3.6m $\times$ 3m) was selected in this study. A five-day indoor air temperature profile from the smart in-home sensor is used for the model identification. The identification results are:  $C_w = 2,220,800$  J/K,  $C_i = 225,440$  J/K,  $C_m = 30,585,600$  J/K,  $R_{win} = 0.0450$  K/W,  $R_w = 0.0478$  K/W,  $R_{wo} = 0.0023$  K/W,  $R_{wi} = 0.0074$  K/W,  $R_{im} = 0.0009$  K/W. With the identified

values of  $R$  and  $C$ , the next five-day indoor air temperature profile is predicted and then compared with the sampled data. Fig. 4 shows the sampled and modeled data of the indoor air temperature during the model training and validation sessions. Predicted results show that the room thermal model is able to predict the indoor air temperature in a relatively high degree of accuracy.

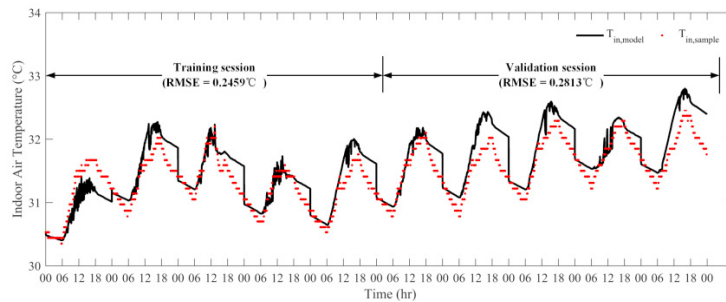


Fig. 4. Modeled and sampled indoor air temperature profiles during the training and validation sessions.

#### 4.1.2. Identification of the inverter-driven AC model

A few studies have focused on the experimental study of steady state performances of ACs. Gayeski [16] carried out relatively elaborate performance experiments for a Mitsubishi split-type inverter-driven AC with a rated cooling capacity of 2.5kW. The experimental tests in his work, however, did not contain enough data. Hence a physics-based modeling technique was used to generate the AC performance data under specific operation conditions. To validate the developed model, the performances of the AC are simulated under the same experimental operation conditions, i.e.  $23^{\circ}\text{C} \leq T_{out} \leq 38^{\circ}\text{C}$ ,  $24^{\circ}\text{C} \leq T_{in} \leq 36^{\circ}\text{C}$ , and  $N = [19, 30, 60, 95]$ .

Fig. 5 shows the comparisons between the experimental data and the predicted data using the physics-based modeling technique. Most deviations of the predicted data to the experimental data are in the range of  $\pm 15\%$ . The mean absolute percentage errors (MAPEs) between the predicted and the tested cooling capacity and COP are 5.65% and 11.9%, respectively. Results show that the physics-based model of the inverter-driven AC has a relatively high degree of accuracy.

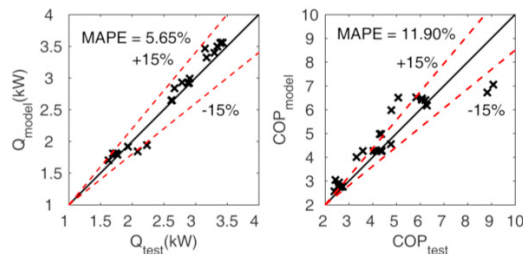


Fig. 5. Comparison between the modeled data and experimental data in Gayeski's work.

## 4.2. Simulation study of AC demand response to dynamic pricing

### 4.2.1 Baseline case

Case studies are carried out on a typical hot summer day. Fig. 6 shows the outdoor weather conditions and internal heat gains from 8:00 to 8:00 on the next day. The room is unoccupied from 8:00 to 18:00 because the occupants are out for school or work during that time. Signals of demand response events, which normally last for 2 to 4 hours, are determined and delivered by the electric utilities. In this study, the DR event is assumed to start from 16:00 to 20:00, which is the time when the residential buildings are occupied and the regional electricity consumption is high. The simulation starts from the 8:00 in the morning, as the room thermal dynamics have been stable for a long time. The initial value of indoor air temperature can then be set as the AC temperature set-point. The time step for simulation is set as 1 minute.

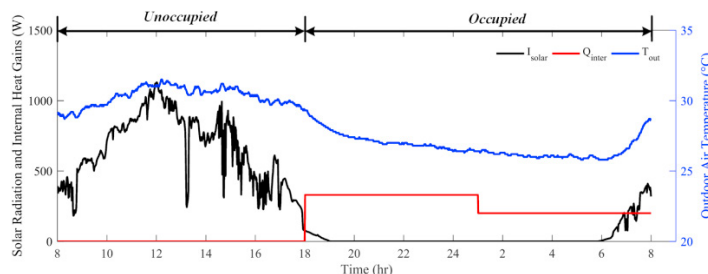


Fig. 6. Outdoor weather conditions and internal heat gains on a typical hot summer day.

To demonstrate the benefits of GA-based load scheduling, a baseline case without any optimization of set-point schedule, is needed for comparison and quantification of the benefits. In the baseline case, the temperature set-point from 18:00 to 24:00 is fixed at 23°C, and the temperature set-point is set 1 degree higher, i.e. 24°C, from 24:00 to the 8:00 on the next day, since during that time of period occupants are normally asleep. The PID controller parameters are tuned manually in the present study with  $K_p = 10$ ,  $K_i = 1$  and  $K_d = 20$ . Profiles of energy consumption, cost and indoor air temperature in the baseline case are plotted in Fig. 7-a - 7-d for comparisons with GA-based cases. The AC automatically switches off for a while around 7:00 in the morning, because the indoor air temperature is lower than the temperature lower threshold 23.5 °C (e.g. the temperature dead-band is 1°C).

#### 4.2.2. Optimization cases

Based on the identified system model, the GA is used to search the optimal temperature set-point schedule. In contrast with the baseline case, the AC is also turned on during the 16:00 to 18:00 to precool the room before the occupants come back from work. The number of the optimized temperature set-points ( $k$ ) and the number of the hourly energy consumption slots ( $m$  in Eq. (12)) are both 16. The number of the indoor air temperature slots ( $n$  in Eq. (13)) and the power consumption slots during the DR hours ( $l$  in Eq. (14)) are 860 and 240, respectively. To satisfy the comfort constraint, the temperature set-point is limited in the range of 22°C - 26°C.

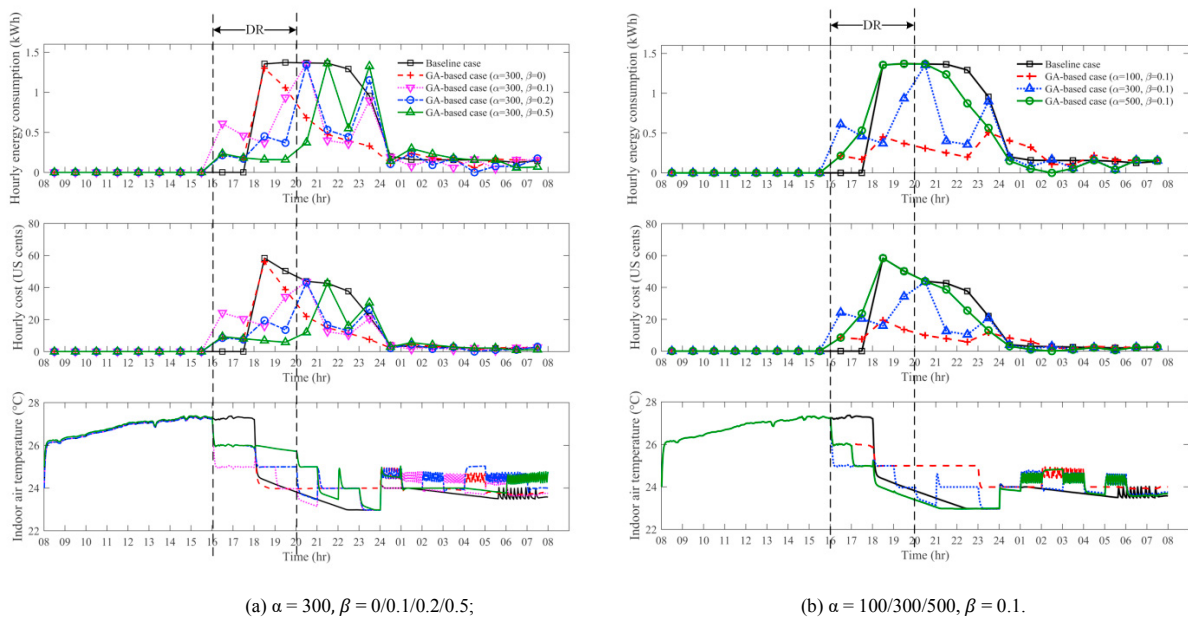


Fig. 7. Profiles of energy consumption, cost and indoor air temperature in the GA-based cases.

The optimal temperature set-point schedule searched by the GA is affected by both the comfort weight  $\alpha$  and the peak power weight  $\beta$ . The cases with different combinations of  $\alpha$  and  $\beta$  are optimized and simulated to show the impacts of the weights on the optimization performances. Fig. 7 shows the profiles of energy consumption, cost and indoor air temperature in the GA-based cases. As shown in Fig. 7-a, when the comfort weight  $\alpha$  is fixed, with the increase of the peak power weight  $\beta$  the peak power consumptions during the DR hours will decrease and the comfort deviations will increase. It can be seen from the Fig. 7-b that when the comfort weight is set higher, the profile of indoor air temperature from 18:00 to 8:00 on the next day is closer to the expected profile. The peak power consumptions during the DR events, however, have certain increases.

## 5. Conclusions

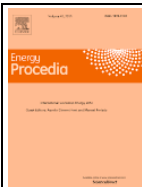
This paper presents a model-based optimal load scheduling method for residential inverter-driven ACs in the presence of dynamic electricity prices. The models of the inverter-driven ACs and room thermal dynamics are developed, identified and integrated for model-based scheduling. The optimization problem is formulated as a mixed integer nonlinear programming problem, which simultaneously takes considerations of the electricity costs, occupant's comfort and peak power consumptions during the DR events. The genetic algorithm is used to effectively solve the optimization problems. Simulation results show that the optimization results, i.e. optimal temperature set-point schedule of the inverter-driven ACs, depend on the preferences of the occupants. The critical weights in the comprehensive objective function play significant roles in the determinations of the resident's tradeoffs between the costs, comfort and peak power demands. The optimal scheduling technique for the residential inverter-driven ACs can be embedded in the programmable communicating thermostats (PCTs) or the smart home energy manage systems (HEMSs) to reduce the electricity bills while maintaining the comfort level of the occupants.

## Acknowledgement

The research work presented in this paper is financially supported by a research grant (G-YBMZ) in the Hong Kong Polytechnic University. The support is gratefully acknowledged.

## References

- [1] Haider HT, See OH, Elmenreich W. A review of residential demand response of smart grid. *Renewable and Sustainable Energy Reviews*. 2016;59:166-78.
- [2] Tang R, Wang S, Gao D-C, Shan K. A power limiting control strategy based on adaptive utility function for fast demand response of buildings in smart grids. *Science and Technology for the Built Environment*. 2016;22:810-9.
- [3] Cui B, Gao D-c, Xiao F, Wang S. Model-based optimal design of active cool thermal energy storage for maximal life-cycle cost saving from demand management in commercial buildings. *Applied Energy*. 2017;201:382-96.
- [4] Kang J, Wang S, Gang W. Performance of distributed energy systems in buildings in cooling dominated regions and the impacts of energy policies. *Applied Thermal Engineering*. 2017;127:281-91.
- [5] Federal Energy Regulatory Commission. A national assessment of demand response potential. 2009.
- [6] Thomas AG, Jahangiri P, Wu D, Cai C, Zhao H, Aliprantis DC, et al. Intelligent residential air-conditioning system with smart-grid functionality. *Smart Grid, IEEE Transactions on*. 2012;3:2240-51.
- [7] Chen Z, Wu L, Fu Y. Real-time price-based demand response management for residential appliances via stochastic optimization and robust optimization. *Smart grid, IEEE transactions on*. 2012;3:1822-31.
- [8] Li S, Zhang D, Roget AB, O'Neill Z. Integrating home energy simulation and dynamic electricity price for demand response study. *Smart Grid, IEEE Transactions on*. 2014;5:779-88.
- [9] Molina D, Lu C, Sherman V, Harley RG. Model predictive and genetic algorithm-based optimization of residential temperature control in the presence of time-varying electricity prices. *Industry Applications, IEEE Transactions on*. 2013;49:1137-45.
- [10] He X-D, Liu S, Asada HH. Modeling of Vapor Compression Cycles for Multivariable Feedback Control of HVAC Systems. *Journal of Dynamic Systems, Measurement, and Control*. 1997;119:183-91.
- [11] Rasmussen BP, Alleyne AG. Control-Oriented Modeling of Transcritical Vapor Compression Systems. *Journal of Dynamic Systems, Measurement, and Control*. 2004;126:54-64.
- [12] Zakula T, Gayeski NT, Armstrong PR, Norford LK. Variable-speed heat pump model for a wide range of cooling conditions and loads. *HVAC&R research*. 2011;17:670-91.
- [13] Zhou R, Zhang T, Catano J, Wen JT, Michna GJ, Peles Y, et al. The steady-state modeling and optimization of a refrigeration system for high heat flux removal. *Applied Thermal Engineering*. 2010;30:2347-56.
- [14] Hu M, Xiao F. Investigation of the Demand Response Potentials of Residential Air Conditioners Using Grey-box Room Thermal Model. *Energy Procedia*. 2017;105:2759-65.
- [15] Hu M, Xiao F, Wang L. Investigation of demand response potentials of residential air conditioners in smart grids using grey-box room thermal model. *Applied Energy*. 2017.
- [16] Gayeski NT. Predictive pre-cooling control for low lift radiant cooling using building thermal mass: Massachusetts Institute of Technology; 2010.



## Biography

The corresponding author is Associate Professor of Department of Building Services Engineering in the Hong Kong Polytechnic University. Research interests include building energy management, optimal and robust control of air-conditioning systems, dynamic simulation of building systems, etc.